JB
Journals.ASM.org

A Novel Component of the *Rhodobacter sphaeroides* Fla1 Flagellum Is Essential for Motor Rotation

Victor Ramírez-Cabrera,[a] Sebastian Poggio,[a] Clelia Domenzain,[a] Aurora Osorio,[a] Georges Dreyfus,[b] and Laura Camarena[a]

Instituto de Investigaciones Biomédicas[a] and Instituto de Fisiología Celular,[b] Universidad Nacional Autónoma de México, Mexico City, Mexico

Here we describe a novel component essential for flagellar rotation in *Rhodobacter sphaeroides*. This protein is encoded by *motF* (RSP_0067), the first gene of a predicted transcriptional unit which contains two hypothetical genes. Sequence analysis indicated that MotF is a bitopic membrane-spanning protein. Protease sensitivity assays and green fluorescent protein (GFP) fusions confirmed this prediction and allowed us to conclude that the C terminus of MotF is located in the periplasmic space. Wild-type cells expressing a functional GFP-MotF fusion show a single fluorescent focus per cell. The localization of this protein in different genetic backgrounds allowed us to determine that normal localization of MotF depends on the presence of FliL and MotB. Characterization of a Δ*motF* pseudorevertant strain revealed that a single nucleotide change in *motB* suppresses the Mot$^-$ phenotype of the *motF* mutant. Additionally, we show that MotF also becomes dispensable when other mutant alleles of *motB* previously isolated as second-site suppressors of Δ*fliL* were expressed in the *motF* mutant strain. These results show that MotF is a new component of the Fla1 flagellum, which together with FliL is required to promote flagellar rotation, possibly through MotB.

The bacterial flagellum is a complex rotating nanomachine that is powered by the proton motive force (7, 63, 67). At the base of this structure, a motor drives flagellar rotation (10, 64). The rotor of the flagellum includes the basal body, the hook, and the flagellar filament. The MotA/MotB complex, or flagellar stator, is embedded in the membrane and is anchored to the peptidoglycan layer through a binding domain present at the C terminus of MotB (54). MotA has four transmembrane helices (TM1 to TM4), with short periplasmic loops between TM1-TM2 and TM3-TM4 and a large cytoplasmic domain between TM2 and TM3 (9, 18, 77). It has been shown that charged residues located in this large cytoplasmic loop are required to generate torque (76). MotB has a short N-terminal cytoplasmic region, a single TM helix, and a large periplasmic domain (14). It has been proposed that the single TM helix of MotB and TM3 and TM4 of MotA form a functional proton channel. The stoichiometry of the functional complex has been shown to be 4 MotA and 2 MotB (11, 12). Recently, it has been estimated that at least 11 $MotA_4/MotB_2$ complexes are arranged around the flagellar rotor (55). It has also been shown that the active MotA/MotB complexes located around the flagellar motor are exchanged rapidly with a membrane pool of inactive stator complexes (37). Activation of the stator complexes involves conformational changes in the periplasmic region of MotB that allow the exposure of the peptidoglycan binding sites as well as the opening of the proton channel. The first event requires unfolding of a short region of MotB known as the linker. The second event requires that the plug domain (an amphipathic alpha-helix located immediately after the TM domain of MotB) stand up, perpendicular to the membrane, to open the proton channel (26, 33, 38, 46). The molecular events that trigger these changes are still not well understood.

On the cytoplasmic side of the flagellar basal body, a structure known as the C-ring is essential for controlling the direction of flagellar rotation and for torque generation (41, 71). This structure is composed of three proteins, FliM, FliN, and FliG (21, 22, 47, 74, 75). The C-terminal domain of FliG contains several charged residues that interact with the charged residues located in the large cytoplasmic loop of MotA (78). It has been shown that the electrostatic interactions between these amino acids are important for torque generation (40, 76, 78).

The bacterial flagellum rotates by using the proton motive force. It has been proposed that the coupling between ion flow through the MotAB channel and flagellar rotation is mediated by conformational changes in MotA that occur by rounds of protonation and deprotonation of the conserved residue Asp32 of MotB. Changes in the cytoplasmic loop of MotA affect torque generation through electrostatic interactions with the C-terminal domain of FliG (13, 31, 32, 79).

In many *Vibrio* species, flagellar rotation depends on Na^+ ions rather than protons (19, 24, 27, 68, 72). In these species, the stator proteins are known as PomA and PomB. The structure of these proteins is similar to that of their counterparts MotA and MotB (3, 70, 73). However, flagellar rotation requires two additional periplasmic proteins, MotX and MotY (42, 43, 45). These proteins are required to incorporate PomA/PomB into the flagellar motor and do not have counterparts in the flagella of *Escherichia coli* and *Salmonella enterica* (34, 39, 66).

The requirement of additional components for flagellar rotation has also been observed in other bacterial species. In *Sinorhizobium meliloti*, the periplasmic protein MotC regulates the rotation speed by acting on MotB (48), and in *Campylobacter jejuni*, the outer membrane protein FlgP (Cj1026c) is essential for flagellar rotation (62).

Rhodobacter sphaeroides is an alphaproteobacterium with two full sets of flagellar genes. One of these sets (Fla1) is constitutively expressed under laboratory growth conditions. This flagellar set was acquired through an event of horizontal transfer. The second

Received 15 May 2012 **Accepted** 5 September 2012
Published ahead of print 7 September 2012
Address correspondence to Laura Camarena, rosal@unam.mx.
Supplemental material for this article may be found at http://jb.asm.org/.

doi:10.1128/JB.00850-12

flagellar set is expressed only in mutant strains that have been selected to swim in the absence of Fla1 (49).

The proteins encoded by the flagellar genes that belong to Fla1 assemble a subpolar flagellum that rotates in a stop-start fashion (2). Flagellar rotation is dependent on the H^+ gradient and requires MotA and MotB (1, 57, 58). Recently, we reported that FliL is also required for flagellar rotation in this bacterium, and it was proposed that FliL modifies the conformation of MotB indirectly (65).

In this work, we identify a novel membrane protein that is essential for flagellar rotation. This protein is recruited to the flagellar base but seems to require a complete motor and/or opening of the MotB plug to stabilize its localization. Genetic evidence supports a possible relationship between this protein and MotB. We propose that the protein encoded by RSP_0067 (*motF*) is an additional component of the flagellar motor that indirectly controls flagellar rotation through MotB.

MATERIALS AND METHODS

Plasmids, bacterial strains, and growth conditions. Bacterial strains and plasmids used in this work are listed in Table 1. *R. sphaeroides* WS8 (61) was grown at 30°C in Sistrom's minimal medium (60) under phototrophic or photoheterotrophic conditions. *E. coli* strains were grown in Luria-Bertani medium (4) at 37°C. Antibiotics were used at the following concentrations: 25 μg/ml kanamycin, 50 μg/ml spectinomycin, and 1 μg/ml tetracycline for *R. sphaeroides* and 100 μg/ml ampicillin, 50 μg/ml kanamycin, 10 μg/ml tetracycline, 30 μg/ml gentamicin, and 50 μg/ml spectinomycin for *E. coli* cultures. *Saccharomyces cerevisiae* was grown in YPDA culture medium (1% yeast extract, 2% peptone, 2% dextrose, and 0.003% adenine) or synthetic defined (SD) minimal medium (Clontech) with various supplements.

Isolation of mutant strains. Amplification of *motF* was carried out by PCR using the oligonucleotides RSP_0067F and RSP_0067R. The resulting 808-bp product was cloned into pTZ19R SacI$^-$, previously digested with XbaI and BamHI (pTZ_motF). The *aadA* gene encoding aminoglycoside 3′-adenyltransferase was amplified by PCR, as an internal portion of the omega-Spc^r (Ω-Spc^r) cassette (44), which removed the known transcriptional termination signals. This fragment was cloned into the unique SacI site present in RSP_0067. The DNA fragment carrying the *motF*::*aadA* allele was then subcloned into the suicide vector pJQ200mp18 (53) and mobilized into WS8 by conjugation (17) with the S17-1 strain (59). The Spc^r Gm^s transconjugants were selected, and the allelic exchange was confirmed by PCR. Strain VR2 (*motF*::*aadA* Δ*motB1*::Kan) was isolated by introducing the Δ*motB1*::Kan allele (65) into strain VR1. To isolate the VR5 strain, a PCR was carried out using the oligonucleotides RSP_6092mut Fwd and RSP_6092 Rvs. The amplification product of 1,591 bp expands from the first half of RSP_0067 to the end of *rpoN2*. The PCR product was cloned into pTZ19R Pst$^-$. The *aadA* gene was cloned into the PstI sites both present in RSP_6092. The resultant allele, RSP_6092::*aadA*, was subcloned into pJQ200mp18 and mobilized into WS8 by conjugation. The Spc^r Gm^s transconjugants were selected, and the allelic exchange was confirmed by PCR.

Motility assays. Sistrom's minimal medium plates with 0.25% agar were inoculated with a 5-μl sample of culture in stationary phase. After 30 h of incubation at 30°C, swimming was evaluated.

Plasmid constructs used in this study. Strain VR1 was complemented using pRK415_motF or pRK415_motFinv. These plasmids were obtained by cloning into pRK415 (30) the amplification products obtained from a PCR using oligonucleotides RSP_0067F and RSP_0067R or 0067FwBam and 0067RvHind, respectively. Internal deletions of *motF* were obtained by inverse PCR, using pTZ19R-motF as the template and the oligonucleotides NoCC67FwdBglII and NoCCRvsBglII or the pair 67co 2-1 and 67co 2-2. The resultant plasmids were digested with XbaI and BamHI, and the appropriate DNA fragments were subcloned into pRK415 to obtain pRK_Δ*motF3* and pRK_Δ*motF4*. To obtain pBB_0067prom, a PCR product of 455 bp, generated with the oligonucleotides RSP_0067 1prom and RSP_0067 2prom, was cloned into pBBMCS53, which carries the reporter gene *uidA* (23). To construct pRK_*gfp-motF*, the amplification products of *gfp* and *motF* obtained from PCRs using the oligonucleotides GFP-67(SD-GFP)FwdHindIII and GFP-67rvs(-stop)XbaI for *gfp* and 0067fwd(faseGFP-M)XbaI and 0067rvs (EcoRI) for *motF* were cloned simultaneously into pRK415 previously digested with HindIII and EcoRI. To obtain pRK_*motF-gfp*, *motF* was amplified using the oligonucleotides RSP_0067F and 0067GFPNcol-Rv; this product was cloned into plasmid pEGFP (Clontech) previously digested with HindIII and NcoI. The fragment carrying the fusion *motF-gfp* was subcloned into pRK415 as a HindIII-EcoRI fragment. pMG_motB was constructed by cloning into pMG171 (28) a 1.7-kb fragment obtained from pRK-motB (65). In this construction *motB* is expressed from the *lac* promoter (*lacp*) present in pMG171. To isolate the *motB* allele encoding MotB D40A, we followed the Stratagene quick-change mutagenesis protocol, using the oligonucleotides motB D40A1 and motB D40A2. The presence of the desired mutation was confirmed by sequencing.

Microscopy. Slides were covered with an agarose pad containing Sistrom's culture medium. A 2-μl drop of an exponentially growing culture was placed on the pad and observed by epifluorescence microscopy. Images were taken with a Hamamatsu Orca-ER camera and a Nikon E600 microscope. Flagellum was stained with 4′,6-diamidino-2-phenylindole (DAPI) according to the previously reported protocol (36). Briefly, a sample of an exponential-phase growing culture was fixed with 3% formaldehyde in phosphate buffer (30 mM final concentration) for 30 min at room temperature. After this period, a final concentration of 1.5 μg/ml DAPI was added and the sample was incubated for 15 min at room temperature. Stained cells were observed by fluorescence microscopy. For electron microscopy, a sample of an overnight culture was washed and stained with 1% uranyl acetate for 5 s and observed at 80 kV with a JEM-1200EXII JEOL electron microscope.

β-Glucuronidase activity. β-Glucuronidase was determined from sonicated cell extracts using 4-methylumbelliferyl-β-D-glucuronide as the substrate and following the published procedure (29). 4-Methylumbelliferone was used as a standard. Specific activities are expressed as nmol of 4-methylumbelliferone/min/mg of protein and are the mean values of three independent cultures, with standard deviations of <15%.

Analysis of the primary sequence of MotF. The sequence of MotF was analyzed using the TOPCONS server (http://topcons.cbr.su.se/) (8), COILS (http://www.ch.embnet.org/software/COILS_form.html), and the Jpred3 server (http://www.compbio.dundee.ac.uk/www-jpred/) (15).

Protease assay. *R. sphaeroides* cells growing exponentially (optical density at 600 nm [OD_{600}] of 0.8) were harvested by centrifugation at 12,000 × *g* for 5 min at 4°C. Cells were washed twice with 10 mM Tris-HCl (pH 7) and resuspended in 500 μl of 100 mM Tris-HCl–20% sucrose. At this point, a sample was taken as a control (50 μl). Spheroplasts were obtained by the addition of EDTA and lysozyme (final concentrations of 50 μM and 0.1 mg/ml, respectively). After 15 min of incubation at 37°C, the cell suspension was divided in two, and 100 mM Tris-HCl buffer (pH 7) or proteinase K at a final concentration of 100 μg/ml was added. These reaction mixtures were incubated at 37°C for 10 min and 20 min. To stop the reaction, phenylmethylsulfonyl fluoride (PMSF; 5 mM) and a 1× protease inhibitor cocktail (complete, mini, EDTA-free protease inhibitor cocktail tablets; Roche) were added. The samples were further incubated for 10 min before being boiled in 1× Laemmli sample buffer (35). The samples were analyzed by immunoblotting with polyclonal antibodies against the $His_{6\times}$-MotFp (MotFp refers to the periplasmic domain of MotF) protein obtained as described below.

Protein overexpression and purification. The DNA region encoding the periplasmic domain of MotF (residues 75 to 239; named MotFp) was obtained by PCR using the oligonucleotides pBAD-67_{COOH}/PstI_Fwd and pBAD-67/Rvs. The product of this reaction was cloned into pBAD HisC previously digested with PstI and EcoRI. *E. coli*

TABLE 1 Strains and plasmids used in this study

Strain or plasmid	Relevant characteristics	Reference or source
Strains		
E. coli		
LMG194	Protein expression strain	Invitrogen
S17-1	*recA endA thi hsdR* RP4-2-Tc::Mu::Tn*7*	59
TOP10	Cloning strain	Invitrogen
R. sphaeroides		
WS8	Wild-type spontaneous Nal^r	61
FS3	WS8 derivative, Δ*fliL3*::*aadA*	65
FS4	WS8 derivative, Δ*motB1*::Kan	65
LC3	WS8 derivative, Δ*motB*::Ω^{Spc}	Laboratory collection
SP7	WS8 derivative, Δ*rpoN2*::Kan	51
SP12	WS8 derivative, Δ*fleT1*::*aadA*	50
SP13	WS8 derivative, Δ*fleQ1*::Kan	50
SP15	WS8 derivative, Δ*fliA*::Kan	50
SP18	WS8 derivative, *flgC1*::Kan	49
VR1	WS8 derivative, *motF*::*aadA*	This study
VR2	VR1 derivative, Δ*motB*::Kan	This study
VR4	VR1 derivative, $motB_{sup9}$	This study
VR5	WS8 derivative, RSP_6092::*aadA*	This study
Plasmids		
pBAD HisC	Expression vector of His-tagged proteins, Ap^r	Invitrogen
pBBMCS53	Transcriptional *uidA* fusion vector, Gm^r	23
pJQ200mp18	Mobilizable suicide vector, Gm^r	53
pPIRL	Vector that encodes tRNAs for rare codons in bacteria, Cm^r	5
pMG171	Vector used for expression in *R. sphaeroides*, Kan^r	28
pRK415	pRK404 derivative, used for expression in *R. sphaeroides*, Tc^r	30
pTZ19R	Cloning vector, Ap^r, pUC derivative	Pharmacia
pTZ19R $SacI^-$	pTZ19R derivative without SacI site	Laboratory collection
pTZ19R Pst^-	pTZ19R derivative without PstI site	Laboratory collection
pBAD His-motFp	pBAD hisC expressing His6X-MotFp (MotFp, periplasmic domain of MotF)	This study
pBB_0067prom	pBBMCS53 carrying the upstream region of *motF*	This study
pMG_motB	pMG171 derivative, expressing wild-type MotB, Kan^r	This study
pMG_motB D40A	pMG171 derivative expressing MotB D40A, Kan^r	This study
pRK_gfp-motF	pRK415 derivative expressing the fusion GFP-MotF	This study
pRK_$motB^+$	pRK415 derivative expressing $motB^+$	65
pRK_motBsup1	pRK415 derivative expressing $motB_{sup1}$ *motB* GCG to GAG (MotB A67E)	65
pRK_motBsup3	pRK415 derivative expressing $motB_{sup3}$ *motB* GCG to GAG (MotB A56E)	65
pRK_motBsup4	pRK415 derivative expressing $motB_{sup4}$ *motB* TTC to TTA (MotB F63L)	65
pRK_motBsup5	pRK415 derivative expressing $motB_{sup5}$ *motB* GCG to GAC (MotB A67D)	65
pRK_motBsup6	pRK415 derivative expressing $motB_{sup6}$ *motB* GCG to ACG (MotB A67T)	65
pRK_motBsup7	pRK415 derivative expressing $motB_{sup7}$ *motB* TTC to CTC (MotB F63L)	65
pRK_motBsup8	pRK415 derivative expressing $motB_{sup8}$ *motB* GCG to GGG (MotB A67G)	65
pRK_motBsup9	pRK415 derivative expressing $motB_{sup9}$ *motB* TCG to CCG (MotB S62P)	This study
pRK415_motF	pRK415 derivative expressing *motF* from the plasmid promoter *lacp*	This study
pRK415_motFinv	pRK415 derivative; *motF* is cloned in the opposite direction of *lacp*	This study
pRK_ΔmotF3	pRK415 derivative Δ*motF3* expressing $MotF\Delta_{29–49}$	This study
pRK_ΔmotF4	pRK415 derivative Δ*motF4* expressing $MotF\Delta_{77–98}$	This study
pRK_motF-gfp	pRK415 derivative expressing the fusion MotF-GFP	This study
pTZ19R_motF	*motF* cloned into pTZ19R $SacI^-$	This study

LMG194/pPIRL was transformed with pBAD His-MotFp. An overnight culture of the resulting strain was diluted 1:100 in fresh medium and incubated at 37°C until it reached an OD_{600} of 0.5. At this point, 2% arabinose was added, and incubation was allowed to proceed for 2 h. Cells were harvested and resuspended in 1/100 of the original culture volume in phosphate-buffered saline (PBS) with 20% glycerol, pH 7.4. Lysozyme was added (1-mg/ml final concentration), and the mixture was incubated for 15 min on ice. The cell suspension was sonicated on ice with a microtip (3 mm), using three bursts of 10 s each. Cell debris was removed by at least three steps of centrifugation (14,000 rpm for 5 min). The supernatant was mixed with nickel-nitrilotriacetic acid (Ni^{2+})-agarose beads (1/250 of the original culture volume) and incubated for 2 h on ice; after this period, the mixture was loaded in a polypropylene column (1 ml) and washed with 50 volumes of PBS buffer and 5 volumes of PBS-20 mM imidazole. The protein was eluted using PBS-200 mM imidazole-20% glycerol, pH 7.4. All washing and elution steps were done under gravity flow.

MotF antibodies. Polyclonal antibodies against $His_{6\times}$-MotFp protein were raised in female BALB/c mice according to previously reported protocols (25).

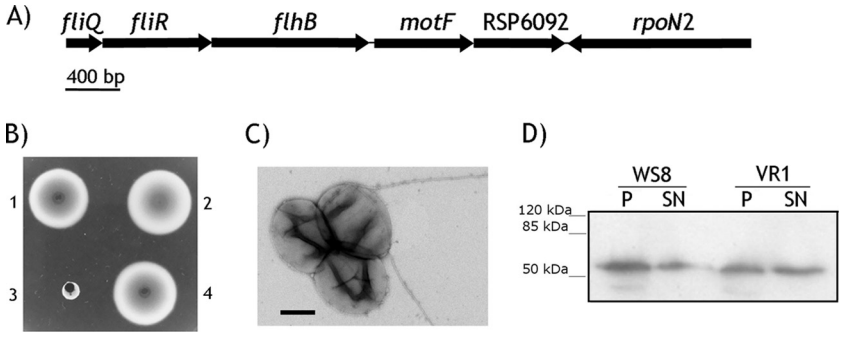

FIG 1 Role of MotF in the flagellar motility of *R. sphaeroides*. (A) Gene arrangement of the flagellar region that contains *motF*, including three genes of the *fliO* operon and two genes downstream of *motF*. The arrows indicate the direction of transcription. (B) Swimming plate inoculated with WS8 (1), the VR5 mutant strain carrying an insertion in RSP_6092 (2), the VR1 mutant strain carrying an insertion in RSP_0067 (*motF*::*aadA*) (3), and VR1 carrying pRK_motF (4). (C) Electron micrograph of VR1 cells showing the presence of flagella. Bar = 500 nm. (D) Western blot analysis of the pellet (P) and supernatant (SN) fractions obtained after strong vortexing of WS8 and VR1 cell cultures. A polyclonal anti-FliC antibody was used for detection.

Oligonucleotides. The sequences of the oligonucleotides used in this work are available upon request.

Immunoblotting. Total cell extracts were subjected to SDS-12% PAGE. Proteins were transferred onto a nitrocellulose membrane. After overnight incubation in 5% nonfat milk-PBS, the membrane was probed with antibody at a dilution of 1:5,000 for anti-MotFp, anti-green fluorescent protein (anti-GFP), or anti-FliH or 1:30,000 for anti-FliC. Incubations were done at room temperature for 2 h. Detection was carried out with a secondary antibody conjugated to alkaline phosphatase (used at a dilution of 1:5,000 and incubated at room temperature for 1 h) and CDP-Star (Applied Biosystems).

RESULTS

MotF is required for flagellar rotation. In the genomic sequence of *R. sphaeroides* 2.4.1, a putative bicistronic operon composed of RSP_0067 and RSP_6092 is located between *flhB* and the gene encoding the flagellar sigma factor, *rpoN*2 (Fig. 1A). A BLAST search using the predicted protein sequence of RSP_0067 showed that this polypeptide is only conserved in other *R. sphaeroides* strains, such as ATCC 17029, ATCC 17025, KD131, and WS8, whereas the protein encoded by RSP_6092 is well conserved in these *R. sphaeroides* strains, and probably in two other bacterial species (i.e., *Octadecabacter antarcticus* 307 and *Loktanella vestfoldensis* SKA53); however, in these two cases the E values are 7e−08 and 0.003, respectively. Due to the genetic context of these genes in the genome of *R. sphaeroides* (Fig. 1A), we decided to determine if they have a role in flagellar motility.

The swimming behavior of RSP_0067 and RSP_6092 mutants was tested in soft-agar plates and by direct observation of liquid cultures under the microscope. Inactivation of RSP_6092 does not affect swimming, even though the protein encoded by this gene can be detected by Western blotting (data not shown). In contrast, inactivation of RSP_0067 impaired swimming severely (Fig. 1B). Accordingly, microscopic observation of liquid cultures showed that inactivation of RSP_0067 yields paralyzed cells. Swimming ability was recovered when this strain was complemented with the wild-type gene cloned in pRK415 (Fig. 1B). In order to clarify if the lack of motility was caused by a defect either in flagellum assembly or in flagellar rotation (Fla$^-$ or Mot$^-$ phenotype), we carried out Western blotting using a polyclonal anti-FliC antibody. Flagellin was detected in the pellet and supernatant of samples that had been subjected to shearing (Fig. 1D), indicating that inactivation of RSP_0067 produces a Mot$^-$ phenotype (cells are able to assemble a flagellum but are unable to rotate it). Electron microscopic observation of RSP_0067 mutant cells corroborated this conclusion (Fig. 1C). Henceforth in this article, RSP_0067 is named *motF*.

The initiation codon of *motF* is located 53 bp downstream from the stop codon of *flhB*. In this intercistronic region, a sequence similar to the σ^{54} consensus promoter was identified (Fig. 2). This sequence matches in 10 out of 11 nucleotides (nt) the σ^{54} consensus promoter (6) (Fig. 2). To determine if this sequence is a functional promoter, a DNA fragment carrying *motF* and 259 bp upstream of the translation start site was cloned in the reverse orientation from the *lac* promoter present in plasmid pRK415. This plasmid restored the swimming ability of VR1 cells (*motF*::*aadA*), suggesting that in this construct, *motF* is transcribed from its own promoter (data not shown).

To determine if this promoter belongs to the flagellar hierarchy of *R. sphaeroides* (50), the upstream region of *motF* was cloned

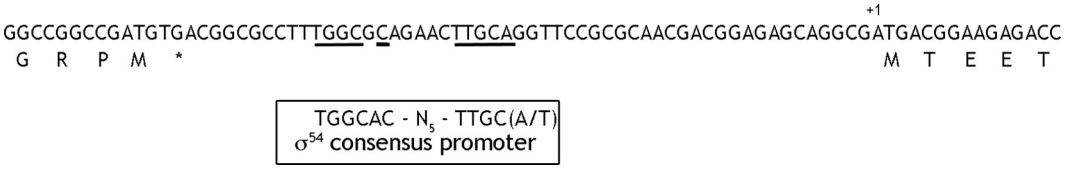

FIG 2 Analysis of the region located upstream of *motF*. Shown is the nucleotide sequence of the intercistronic region between *flhB* and *motF*. Below the nucleotide sequence, on the left, four amino acids corresponding to the C-terminal end of FlhB are shown; the stop codon is indicated with an asterisk. To the right, the first five amino acids corresponding to the N-terminal region of MotF are shown. Above the nucleotide sequence, the "+1" indicates the first base of the ATG initiation codon of MotF. The conserved nucleotides that match the σ^{54} consensus promoter are underlined. Below, in a box, the σ^{54} consensus promoter sequence is shown.

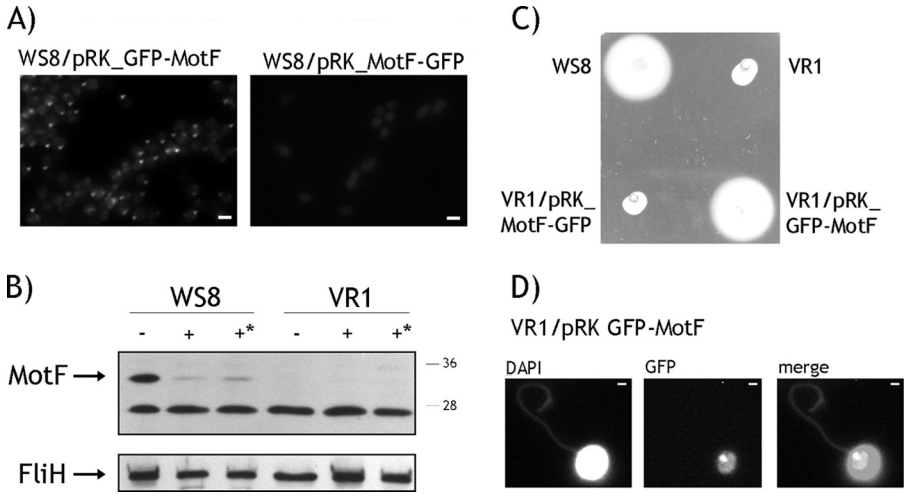

FIG 3 MotF topology. (A) Representative images of WS8 cells expressing GFP-MotF or MotF-GFP. Bar = 2 μm. (B) Western blot analysis of spheroplasts from WS8 and VR1 cells. −, spheroplasts without proteinase K; +, spheroplasts treated with proteinase K for 10 min; +*, spheroplasts treated with proteinase K for 20 min. The protein recognized by the antibody is indicated on the left. (C) Swimming plate inoculated with WS8, VR1, VR1/pRK_motF-gfp, and VR1/pRK_gfp-motF. (D) Example of a characteristic WS8 wild-type cell expressing GFP-MotF. Cells were stained with DAPI to covisualize the flagellum and the signal from GFP-MotF. Bar = 1 μm.

before the *'uidA* reporter gene present in plasmid pBBMCS53 (23). The amount of β-glucuronidase (encoded by *uidA*) produced by the resultant plasmid (pBB_0067prom) was evaluated in different backgrounds.

Briefly, it should be mentioned that the flagellar hierarchy of *R. sphaeroides* has four tiers; at the top, the master regulator FleQ, which is a σ^{54} transcriptional activator, promotes the expression of the *fleT* operon. This operon contains the genes *fleT fliEFGHIJ* and represents class II of the hierarchy. FleT is also a σ^{54} transcriptional activator that together with FleQ is required for the expression of class III genes. In class III, the genes encoding the rest of the components of the basal body, the export apparatus, the hook, the motor proteins (MotA and MotB), the σ^{28} factor, and the anti-sigma, FlgM, are found. Flagellin encoded by *fliC* is transcribed by a σ^{28}-dependent promoter and represents class IV of the hierarchy (50).

Plasmid pBB_0067prom was introduced to the wild-type strain as well as the SP13 (Δ*fleQ1*::Kan), SP12 (Δ*fleT1*::*aadA*); SP15 (Δ*fliA*::Kan), and SP7 (Δ*rpoN2*::Kan) strains. The amounts of β-glucuronidase were 20.7, 60.8, and 124.6-fold higher in the wild-type strain than in SP12, SP13, and SP7, respectively. In contrast, a 4.3-fold increment was observed in strain SP15 (Δ*fliA*::Kan) with respect to the WS8 wild-type strain. This result is in agreement with recent evidence showing that the expression of class III flagellar genes is increased in a strain lacking the σ^{28} factor (69). From these results, we suggest that *motF* is expressed from its own promoter that belongs to flagellar class III.

MotF is a bitopic membrane protein with the majority of its sequence in the periplasm. *motF* encodes a polypeptide of 239 amino acids. Analysis of the primary sequence of MotF predicts a transmembrane (TM) segment that runs from residues 54 through 74. The topology of MotF in the inner membrane was tested by following two independent experimental approaches. In one of them, GFP was fused to the N- or C-terminal region of MotF. Observation of WS8 or VR1 (*motF*::*aadA*) cells expressing GFP-MotF or MotF-GFP from the *lac* promoter of pRK415 revealed the presence of a single fluorescent focus per cell generated by the N-terminal GFP-MotF fusion but not by the C-terminal MotF-GFP fusion (Fig. 3A). Given that GFP is fluorescent only in the cytoplasm and not in the periplasmic space (16, 20), we concluded that the C terminus of MotF is located in the periplasmic side of the membrane. To corroborate this result, we carried out a protease sensitivity assay. In this assay, spheroplasts were incubated in the presence or absence of proteinase K; after incubation, the samples were analyzed by Western blotting. Figure 3B shows that in the presence of proteinase K, the band corresponding to MotF disappears. The identity of the unspecific band recognized by the MotF antibody is unknown, but it should correspond to a cytoplasmic protein given that its presence is not affected by the action of proteinase K. As a control, we analyzed the same samples by Western blotting using an anti-FliH antibody. The presence of FliH in all the samples indicates that the spheroplasts were intact and proteolysis was restricted only to the proteins exposed to the outer side of the internal membrane. These results corroborate that the C terminus of MotF is located in the periplasmic side of the membrane. In addition, as shown in Fig. 3C, GFP-MotF was able to restore the swimming ability of strain VR1, strongly suggesting that GFP-MotF is a functional protein.

To determine if the fluorescent focus generated by GFP-MotF colocalizes with the flagellar structure, we stained the flagellar filament with DAPI, and it was visualized by fluorescence microscopy. Merged images of GFP-MotF and stained flagellar filaments revealed that GFP-MotF is commonly localized with what seems to be the base of the flagellum (Fig. 3D).

Localization of MotF depends on the presence of a complete motor and/or the opening of the MotB plug. The localization pattern of GFP-MotF was evaluated in different genetic backgrounds. No fluorescent foci were observed when a plasmid expressing GFP-MotF was introduced into SP12 (Δ*fleT1*::*aadA*) and SP13 (Δ*fleQ1*::Kan) strains (Fig. 4A). Given that the amount of GFP-MotF detected in these strains by Western blotting was similar to that detected for the VR1 (*motF*::*aadA*) strain (Fig. 4B), we

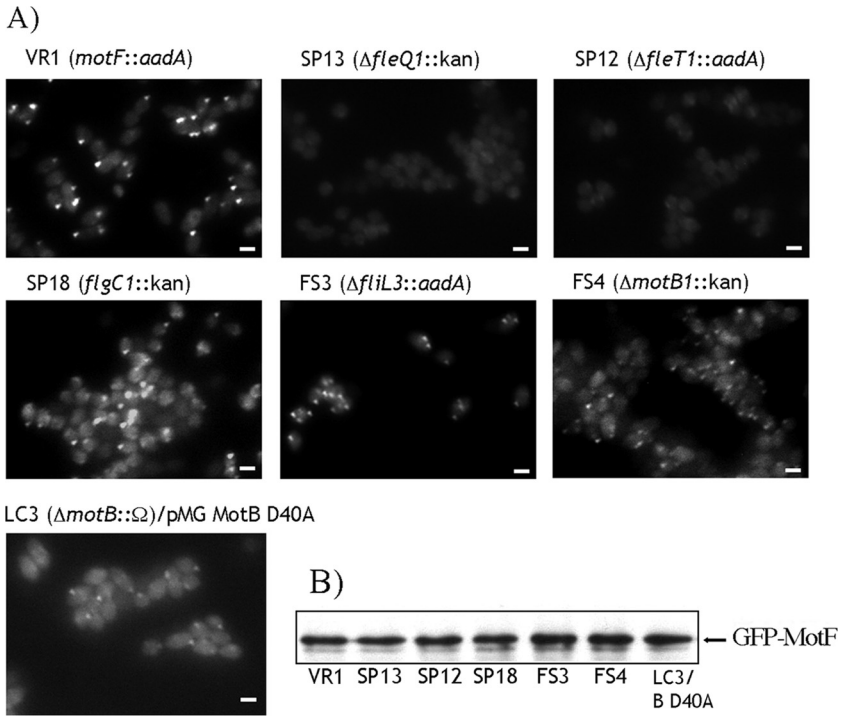

FIG 4 GFP-MotF localization in different genetic backgrounds. (A) Representative images of different strains expressing GFP-MotF: VR1 (*motF*::*aadA*), SP12 (Δ*fleT1*::*aadA*), SP13 (Δ*fleQ1*::Kan), SP18 (*flgC1*::Kan), FS3 (Δ*fliL3*::*aadA*), FS4 (Δ*motB1*::Kan), and LC3 (Δ*motB*::Ω^{Spc})/pMG_motB D40A. Bar = 2 μm. (B) Western blot of GFP-MotF expressed in different strains. Total cell extracts of each strain were tested by Western blotting using a mouse polyclonal anti-GFP antibody.

concluded that GFP-MotF requires at least another flagellar protein to be localized.

Since MotF is required for flagellar rotation, we tested if other proteins with a similar function were required in order to observe GFP-MotF as a single focus in the cell (as observed in WS8 or VR1 [*motF*::*aadA*] strains [Fig. 3A and 4A, respectively]). Surprisingly, for the Mot$^-$ FS3 (Δ*fliL3*::*aadA*) and FS4 (Δ*motB1*::Kan) strains, two or three GFP-MotF fluorescent foci per cell were frequently detected (Fig. 4A). For the WS8 and VR1 strains, approximately 80% of the cells showed a single fluorescent focus, whereas the remaining 20% did not have any fluorescent foci or showed two low-intensity foci localized in the middle of the cell. When GFP-MotF was expressed in a mutant with a defect in the flagellar rod (SP18), a reduction in the number of cells with fluorescent signal was noticed; however, when present, a single fluorescent focus was usually observed (Fig. 4A). In contrast, for FS3 and FS4, only 30% of the cells have a single focus, whereas the majority of the cells showed two or three fluorescent foci per cell (Fig. 4A).

Since GFP-MotF showed an abnormal localization pattern in the Mot$^-$ strains tested, we determined its localization in a Mot$^-$ strain that still had all the motor components. For this, a *motB* allele was generated in which the codon for the conserved aspartic acid required for proton transport was changed to alanine (MotB D40A). The same mutation has been reported to produce a Mot$^-$ phenotype in *E. coli* (79). This *motB* mutant allele was unable to complement a Δ*motB*::Ω^{Spc} mutant (data not shown). Observation of GFP-MotF in the LC3 (Δ*motB*::Ω^{Spc}) strain expressing MotB D40A showed a single fluorescent focus per cell (Fig. 4A).

A Western blot assay showed that the amounts of GFP-MotF are similar in all the mutant strains, indicating that the different localization patterns observed are not the result of different levels of GFP-MotF (Fig. 4B). Since GFP-MotF is present in the same amount in the SP18 strain, the reduction in the number of detectable foci in this strain suggests that the rod may be indirectly required to stabilize the localization of GFP-MotF.

Point mutations in *motB* restore swimming in the VR1 (*motF*::*aadA*) strain. To obtain additional information about the role of MotF in flagellar rotation, we selected pseudorevertant strains that restore the swimming ability of VR1. One strain was isolated after incubation of a swimming plate for 1 week. To determine the possible mutation(s) that compensated for the lack of MotF in this strain, we sequenced five genes known to be associated with flagellar rotation in *R. sphaeroides* (i.e., *motA*, *motB*, *fliL*, *fliM*, and *fliN*). Comparison of these sequences with those of the wild-type strain (52) revealed a single point mutation in the *motB* gene. This mutation changes serine 62, which is located immediately after the TM segment, to proline. To confirm that this change was sufficient to promote flagellar rotation in the absence of MotF, we introduced a plasmid expressing either the wild type or MotB S62P (pRK_motB$^+$ or pRK_motBsup9) into a *motF*::*aadA* Δ*motB1*::Kan double mutant (VR2 strain). Swimming was recovered only with the plasmid that expresses the suppressor allele of *motB*, indicating that this change in *motB* is sufficient to bypass the requirement of MotF (Fig. 5A).

We have previously shown that in *R. sphaeroides*, the Mot$^-$ phenotype of a *fliL* mutant strain can be suppressed by secondary mutations that are located in the MotB periplasmic region immediately after the TM segment (65). The fact that the *motF* suppressing mutation lies in the same region prompted us to test if the

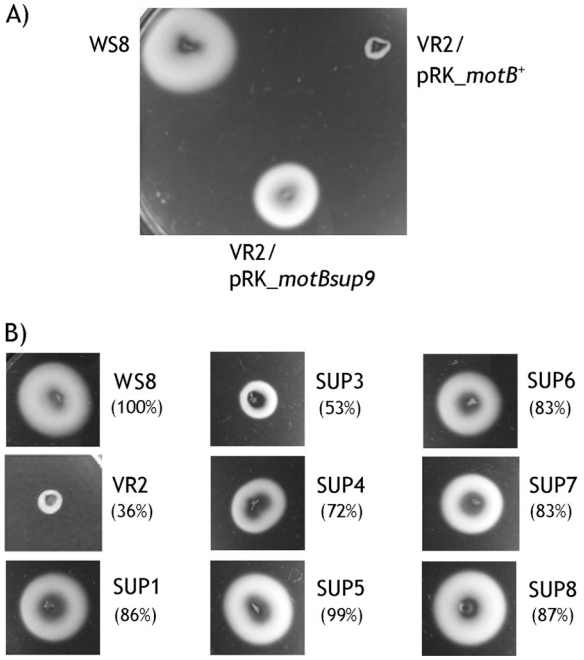

FIG 5 Swimming of second-site suppressor strains. (A) Swimming plate inoculated with WS8 (wild type), VR2/pRK_motB$^+$, and VR2/pRK_motBsup9. (B) Swimming assay testing the suppression of the *motF*::*aadA* mutation by the *motB* alleles isolated as second-site suppressors of Δ*fliL*::*aadA*. SUP1, MotB A67E; SUP3, MotB A56E; SUP4, MotB F63L; SUP5, MotB A67D; SUP6, MotB A67T; SUP7, MotB F63L; SUP8, MotB A67G. Each *motB* allele was tested in the VR2 strain (Δ*motB*::Kan *motF*::*aadA*). The percentages represent the averages of the swimming ring diameters from three different assays. Values are expressed as percentages of the value determined for the WS8 strain.

various *motB* suppressor alleles isolated in the Δ*fliL* background could also compensate for the absence of MotF.

Figure 5B shows that VR2 strain recovered its swimming ability when the different *motB* suppressor mutant alleles were expressed from the *lac* promoter present in pRK415. This result suggests that MotF could control flagellar rotation by affecting directly or indirectly the conformation of MotB.

We observed that the different *motB* suppressor alleles allowed swimming of the VR2 strain with various degrees of proficiency. It should be noted that the expansion of the swarm ring is the result not only of a functional flagellar motor but also of other factors such as a well-tuned chemotactic system and bacterial growth rate. In this assay, we noticed that MotB A56E (SUP3) restored swimming in a minor degree, whereas SUP1 (A67E), SUP5 (A67D), and SUP8 (A67G) allowed better swimming and SUP4 (F63L), SUP7 (F63L), and SUP6 (A67T) were intermediate. It can be hypothesized that the different degrees of complementation by the suppressor alleles may be related to how much the MotB proton channel is allowed to open by each of the substitutions. The most vigorous swimming was detected for substitutions that change A67 (Fig. 5B), suggesting that this residue may be relevant in the interaction between the hydrophobic side of the amphipathic helix and the membrane (see Fig. S1 in the supplemental material). In contrast, the strain expressing MotB A56E (SUP3) was almost unable to move away from the inoculation point, and when observed under the microscope, most of the cells were nonmotile, with approximately only 1% of these cells swimming slowly; some of these cells stopped moving and did not resume swimming during the observation time (approximately 5 s). This could be related to the fact that A56 is located immediately after the TM segment and does not lie in the region presumed to act as a plug for the proton channel; it has also been proposed that this change could affect the plug indirectly by shifting the TM helix or induce a more general conformational change in MotB (65). Interestingly, the same observations were made at the microscopic and macroscopic levels when MotB A56E was used to suppress the absence of FliL (65). In general, the efficiency of suppression seems to be dependent on the conformation that each of the MotB versions acquires rather than on the particular mutation (Δ*fliL* or Δ*motF*) being suppressed.

To evaluate if MotF interacts directly with MotB, we carried out a yeast double-hybrid assay. For this, the periplasmic region of MotF (MotFp) was fused to the activation domain (AD) of GAL4. The interaction of this protein fusion was tested against MotBp (periplasmic domain of MotB) fused to the binding domain (BD) of GAL4. No interaction between MotBp and MotFp was detected. Since *fliL* and *motF* mutants have the same phenotype and are complemented by the same *motB* suppressor alleles, we also tested the interaction between the periplasmic regions of these two proteins in a double-hybrid assay, but no positive interaction was detected.

Functional contribution of two regions located adjacent to the TM domain of MotF. Important conformational changes occur in the periplasmic domain of MotB when the MotA/MotB complex is assembled in the flagellar structure. These changes affect the plug region of MotB, which lies immediately after the TM domain (26). We presumed that these alterations could require another protein to trigger this rearrangement in MotB. Therefore, we tested if a region in the periplasmic side of MotF adjacent to the TM domain could play a relevant role in flagellar rotation. For this purpose, we deleted a region in MotF that contains residues 77 to 98 (Δ*motF4*). In addition, we deleted the region of MotF that lies in the cytoplasmic side before the TM domain (residues 29 to 49) (Δ*motF3*). This region overlaps with a predicted coiled-coil structure.

VR1 cells expressing these versions of MotF showed that MotFΔ_{29-49} (Δ*motF3*) supports swimming less efficiently than the wild type (Fig. 6A). In contrast, MotFΔ_{77-98} (Δ*motF4*) showed a severe reduction of the swarm ring, suggesting that this region is relevant for MotF function (Fig. 6A). Microscopic observation of these mutant cells showed that both MotFΔ_{29-49} (Δ*motF3*) (15 ± 4.6 μm/s) and MotFΔ_{77-98} (Δ*motF4*) (5 ± 0.8 μm/s) showed a slower swimming speed than the wild type (26 ± 3.3 μm/s). A nonmotile strain registered a swimming speed of 1.7 ± 0.8 μm/s, probably due to Brownian motion. A major difference between MotFΔ_{29-49} and MotFΔ_{77-98} was that in a common field of MotFΔ_{77-98}, only a few swimming cells were present (approximately 10%). Western blot assays showed that both mutant proteins are expressed at levels similar to that of the wild-type protein (Fig. 6B).

We also determined the ability of GFP-MotFΔ_{77-98} (Δ*motF4*) to form fluorescent foci. As shown in Fig. 6C, cells expressing GFP-MotFΔ_{77-98} (Δ*motF4*) showed two or more fluorescent foci per cell, similar to what occurs with the GFP-MotF fusion in the FS3 (Δ*fliL3*::*aadA*) and FS4 (Δ*motB1*::Kan) Mot$^-$ strains (Fig. 4A). These results strongly indicate that the region of MotF located between amino acids 77 to 98 is required for swimming

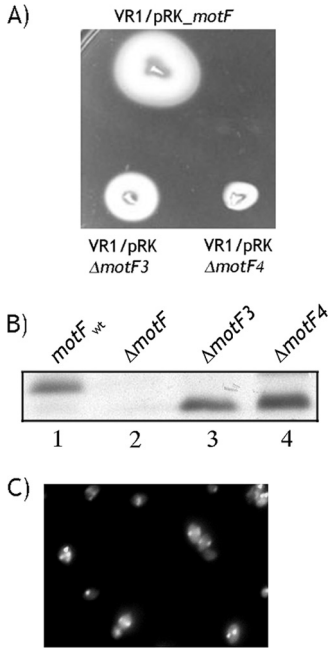

FIG 6 Effect of the MotF region located after the TM region in swimming and MotF localization. (A) Swimming plate inoculated with VR1/pRK_motF and VR1 carrying pRK_ΔmotF3 or pRK_ΔmotF4; (B) Western blot of VR1 cells expressing wild-type MotF (1), VR1 cells expressing MotF without plasmid (2), VR1 expressing MotFΔ_{29-49} (3), and VR1 expressing MotFΔ_{77-98} (4). (C) Representative image of VR1 cells expressing GFP-MotFΔ_{77-98}.

and for the correct localization of MotF. Although MotFΔ_{77-98} is present in a level similar to that of the wild-type protein, it is also possible that the deletion of residues 77 to 98 could affect the overall structure of MotF, thus hindering flagellar rotation.

DISCUSSION

Recent studies with bacterial species other than *E. coli* and *S. enterica* have shown that the flagellar rotor is frequently more complex than originally described. Additional components are frequently present in the flagellar structures of other species. For instance, it has been reported that in *Vibrio alginolyticus* and *Vibrio parahaemolyticus*, MotX and MotY are essential components for the rotation of the Na^+-driven polar flagellum (for review, see references 39 and 67). In *S. meliloti*, the periplasmic protein MotC controls flagellar rotation speed (48). In this work, we report that MotF is a new transmembrane protein that is essential for the rotation of the Fla1 flagellum of *R. sphaeroides*.

MotF is conserved among all sequenced *R. sphaeroides* species; moreover, using MotF as a query sequence in a BLAST search, marine metagenome sequences could be retrieved, suggesting that other, so-far-uncharacterized bacteria may have a gene with a function similar to that of the MotF gene.

The *motF* gene seems to form an operon with the RSP_6092 gene; however, inactivation of RSP_6092 did not affect swimming, suggesting that this gene is irrelevant for swimming under laboratory conditions. The expression of *motF* depends on its own promoter, which our data suggest to be recognized by the RNA polymerase associated with the σ^{54} factor and to be dependent on the σ^{54} activators, FleQ and FleT. This indicates that *motF* belongs to class III of the *R. sphaeroides* flagellar hierarchy (50). As occurs with other class III promoters, the residual transcriptional activity of *motFp* in the absence of FleT is higher than in the absence of FleQ. This has been explained on the basis that FleQ has a higher ATPase activity than FleT. As a consequence, FleQ may remodel the Eσ54 complex more efficiently than FleT, allowing a higher level of residual activity (50).

As mentioned before, flagellar class III includes most of the genes encoding the proteins that form the basal body (except FliE, FliF, and FliG), the hook, and the stator proteins MotA and MotB. *fliL* also belongs to this class, and its product is required for motor functioning in *R. sphaeroides* (50). Presumably, MotF is incorporated to the flagellar structure at the time that the basal body proteins and the MotA/MotB complexes are also being assembled.

Two independent results allow us to conclude that MotF has its largest domain in the periplasm (residues 75 to 239). This topology encouraged us to test if MotFp could interact with FliLp or MotBp, given that both proteins also have large periplasmic domains and are essential for flagellar rotation. Although we could not detect interactions between these proteins, MotF could still interact with FliL and/or the MotA/MotB complex through its TM region. Interestingly, we identified the GXXXG motif in the TM helix of MotF. This motif has been suggested to be relevant in the interaction between TM helices (56). It remains to be tested if this motif mediates the interaction of MotF with other flagellar proteins.

We characterized the localization pattern of GFP-MotF in different genetic backgrounds, with the idea that a change in MotF localization could allow us to identify a potential interacting partner in the flagellar structure. MotF was not localized in strains that do not express the class II or III genes (as occurs in strains SP12 and SP13), supporting the idea that MotF is recruited to the flagellar structure through its interaction with a protein that should belong to class III in the flagellar transcriptional hierarchy. Similarly, it was previously shown that the localization of GFP-FliL is dependent on the presence of FleQ and FleT (65).

Given the similar topology and function of MotF, MotB, and FliL, we tested if the localization of GFP-MotF was dependent on the presence of these two other proteins. GFP-MotF showed a single fluorescent focus in the wild-type or SP18 (*flgC1*::Kan) strain; surprisingly, multiple GFP-MotF fluorescent foci were detected in the absence of FliL or MotB. This result suggests that although these proteins are required for normal localization of MotF, an additional flagellar class III protein is responsible for MotF clustering and consequently for the formation of multiple foci in the *motB* and *fliL* mutant strains.

Why are FliL and MotB required for the normal localization of MotF? A possible clue comes from the fact that the *fliL* and *motB* mutant strains have a Mot^- phenotype. It is possible that, besides the hypothetical flagellar class III protein required for MotF clustering, a functional motor is required to stabilize MotF around the flagellar structure, resulting in a single GFP-MotF focus. To test this idea, we expressed the GFP-MotF protein in a strain in which the wild-type MotB protein was replaced with a nonfunctional MotB version (MotB D40A). In this case, GFP-MotF formed a single focus per cell. This result indicates that MotF recruitment to the flagellar structure requires not a functional motor, as we initially hypothesized, but the simultaneous presence of FliL, the MotA/MotB complex, and/or the MotB protein that has acquired the open channel conformation. The requirement of an open channel for MotF localization is supported by the observation that

GFP-MotF is present as a single fluorescent focus in the absence of FliL provided that a *motB* suppressor allele is also present (data not shown).

We previously reported that in *R. sphaeroides*, FliL is essential for flagellar rotation; we isolated several strains carrying *motB* point mutations that allow rotation in the absence of FliL (65). All these mutations were found to be in the region that has been proposed to act as a plug for the proton channel (26, 65). It has been proposed that this region keeps the MotA/MotB proton channel closed until MotB is incorporated to the flagellar structure (26). Since we previously observed that the periplasmic regions of MotB and FliL do not interact, it was proposed that FliL could participate indirectly in the control of the proton channel opening (65). In this work, it is shown that MotF is also dispensable for flagellar rotation provided that the point mutant alleles of *motB* that presumably keep the proton channel open are being expressed. Therefore, we propose that both FliL and MotF participate in the process that activates or keeps the MotA/MotB proton channel open.

From our results, it could be envisioned that in *R. sphaeroides*, another flagellar protein might exist that interacts with FliL, MotF, and MotB. FliL and MotF may regulate MotB through this hypothetical protein.

The elucidation of new components of the flagellar motor of *R. sphaeroides* will provide useful information that will undoubtedly expand our view on the different ways in which a molecular machine can be controlled.

ACKNOWLEDGMENTS

We thank Teresa Ballado, Javier de la Mora, and Georgina Diaz Herrera for technical assistance. We also thank the IFC Molecular Biology Unit for sequencing facilities as well as Yael González and the Microscopy Unit for the electron micrographs.

This work was supported in part by grants from the Consejo Nacional de Ciencia y Tecnología (SEP-CONACYT 106081) and DGAPA/UNAM (IN206811-3).

REFERENCES

1. **Armitage JP, Evans MCW.** 1985. Control of the protonmotive force in *Rhodopseudomonas sphaeroides* in the light and dark and its effect on the initiation of flagellar rotation. Biochim. Biophys. Acta **806**:42–55.
2. **Armitage JP, Macnab RM.** 1987. Unidirectional, intermittent rotation of the flagellum of *Rhodobacter sphaeroides*. J. Bacteriol. **169**:514–518.
3. **Asai Y, et al.** 1997. Putative channel components for the fast-rotating sodium-driven flagellar motor of a marine bacterium. J. Bacteriol. **179**: 5104–5110.
4. **Ausubel FM, et al.** 1987. Current protocols in molecular biology, vol 1. John Wiley & Sons, Inc., New York, NY.
5. **Bao K, Cohen SN.** 2001. Terminal proteins essential for the replication of linear plasmids and chromosomes in *Streptomyces*. Genes Dev. **15**:1518–1527.
6. **Barrios H, Valderrama B, Morett E.** 1999. Compilation and analysis of σ^{54}-dependent promoter sequences. Nucleic Acids Res. **27**:4305–4313.
7. **Berg HC.** 2003. The rotary motor of bacterial flagella. Annu. Rev. Biochem. **72**:19–54.
8. **Bernsel A, Viklund H, Hennerdal A, Elofsson A.** 2009. TOPCONS: consensus prediction of membrane protein topology. Nucleic Acids Res. **37**:W465–W468.
9. **Blair DF, Berg HC.** 1991. Mutations in the MotA protein of *Escherichia coli* reveal domains critical for proton conduction. J. Mol. Biol. **221**:1433–1442.
10. **Blair DF, Berg HC.** 1990. The MotA protein of *E. coli* is a proton-conducting component of the flagellar motor. Cell **60**:439–449.
11. **Braun TF, Al-Mawsawi LQ, Kojima S, Blair DF.** 2004. Arrangement of core membrane segments in the MotA/MotB proton-channel complex of *Escherichia coli*. Biochemistry **43**:35–45.
12. **Braun TF, Blair DF.** 2001. Targeted disulfide cross-linking of the MotB protein of *Escherichia coli*: evidence for two H(+) channels in the stator complex. Biochemistry **40**:13051–13059.
13. **Che YS, Nakamura S, Kojima S, Kami-ike N, Namba K, Minamino T.** 2008. Suppressor analysis of the MotB(D33E) mutation to probe bacterial flagellar motor dynamics coupled with proton translocation. J. Bacteriol. **190**:6660–6667.
14. **Chun SY, Parkinson JS.** 1988. Bacterial motility: membrane topology of the *Escherichia coli* MotB protein. Science **239**:276–278.
15. **Cole C, Barber JD, Barton GJ.** 2008. The Jpred 3 secondary structure prediction server. Nucleic Acids Res. **36**:W197–W201.
16. **Daley DO, et al.** 2005. Global topology analysis of the *Escherichia coli* inner membrane proteome. Science **308**:1321–1323.
17. **Davis J, Donohue TJ, Kaplan S.** 1988. Construction, characterization, and complementation of a Puf$^-$ mutant of *Rhodobacter sphaeroides*. J. Bacteriol. **170**:320–329.
18. **Dean GE, Macnab RM, Stader J, Matsumura P, Burks C.** 1984. Gene sequence and predicted amino acid sequence of the *motA* protein, a membrane-associated protein required for flagellar rotation in *Escherichia coli*. J. Bacteriol. **159**:991–999.
19. **Dibrov PA, Kostryko VA, Lazarova RL, Skulachev VP, Smirnova IA.** 1986. The sodium cycle. I. Na+-dependent motility and modes of membrane energization in the marine alkalotolerant *Vibrio alginolyticus*. Biochim. Biophys. Acta **850**:449–457.
20. **Feilmeier BJ, Iseminger G, Schroeder D, Webber H, Phillips GJ.** 2000. Green fluorescent protein functions as a reporter for protein localization in *Escherichia coli*. J. Bacteriol. **182**:4068–4076.
21. **Francis NR, Irikura VM, Yamaguchi S, DeRosier DJ, Macnab RM.** 1992. Localization of the *Salmonella typhimurium* flagellar switch protein FliG to the cytoplasmic M-ring face of the basal body. Proc. Natl. Acad. Sci. U. S. A. **89**:6304–6308.
22. **Francis NR, Sosinsky GE, Thomas D, DeRosier DJ.** 1994. Isolation, characterization and structure of bacterial flagellar motors containing the switch complex. J. Mol. Biol. **235**:1261–1270.
23. **Girard L, et al.** 2000. Differential regulation of *fixN*-reiterated genes in *Rhizobium etli* by a novel *fixL-fixK* cascade. Mol. Plant Microbe Interact. **13**:1283–1292.
24. **González Y, Venegas D, Mendoza-Hernandez G, Camarena L, Dreyfus G.** 2010. Na(+)- and H(+)-dependent motility in the coral pathogen *Vibrio shilonii*. FEMS Microbiol. Lett. **312**:142–150.
25. **Harlow E, Lane D.** 1988. Antibodies. A laboratory manual. Cold Spring Harbor Laboratory Press, Cold Spring Harbor, NY.
26. **Hosking ER, Vogt C, Bakker EP, Manson MD.** 2006. The *Escherichia coli* MotAB proton channel unplugged. J. Mol. Biol. **364**:921–937.
27. **Imae Y, Atsumi T.** 1989. Na+-driven bacterial flagellar motors. J. Bioenerg. Biomembr. **21**:705–716.
28. **Inui M, Nakata K, Roh JH, Vertes AA, Yukawa H.** 2003. Isolation and molecular characterization of pMG160, a mobilizable cryptic plasmid from *Rhodobacter blasticus*. Appl. Environ. Microbiol. **69**:725–733.
29. **Jefferson RA, Burgess SM, Hirsh D.** 1986. β-Glucuronidase from *Escherichia coli* as a gene-fusion marker. Proc. Natl. Acad. Sci. U. S. A. **83**:8447–8451.
30. **Keen NT, Tamaki S, Kobayashi D, Trollinger D.** 1988. Improved broad-host-range plasmids for DNA cloning in Gram-negative bacteria. Gene **70**:191–197.
31. **Kim EA, Price-Carter M, Carlquist WC, Blair DF.** 2008. Membrane segment organization in the stator complex of the flagellar motor: implications for proton flow and proton-induced conformational change. Biochemistry **47**:11332–11339.
32. **Kojima S, Blair DF.** 2001. Conformational change in the stator of the bacterial flagellar motor. Biochemistry **40**:13041–13050.
33. **Kojima S, et al.** 2009. Stator assembly and activation mechanism of the flagellar motor by the periplasmic region of MotB. Mol. Microbiol. **73**: 710–718.
34. **Kojima S, et al.** 2008. Insights into the stator assembly of the *Vibrio* flagellar motor from the crystal structure of MotY. Proc. Natl. Acad. Sci. U. S. A. **105**:7696–7701.
35. **Laemmli UK.** 1970. Cleavage of structural proteins during the assembly of the head of bacteriophage T4. Nature **227**:680–685.
36. **Lam H, Schofield WB, Jacobs-Wagner C.** 2006. A landmark protein essential for establishing and perpetuating the polarity of a bacterial cell. Cell **124**:1011–1023.

37. **Leake MC, et al.** 2006. Stoichiometry and turnover in single, functioning membrane protein complexes. Nature **443**:355–358.
38. **Li N, Kojima S, Homma M.** 2011. Characterization of the periplasmic region of PomB, a Na+-driven flagellar stator protein in *Vibrio alginolyticus*. J. Bacteriol. **193**:3773–3784.
39. **Li N, Kojima S, Homma M.** 2011. Sodium-driven motor of the polar flagellum in marine bacteria *Vibrio*. Genes Cells **16**:985–999.
40. **Lloyd SA, Blair DF.** 1997. Charged residues of the rotor protein FliG essential for torque generation in the flagellar motor of *Escherichia coli*. J. Mol. Biol. **266**:733–744.
41. **Lloyd SA, Tang H, Wang X, Billings S, Blair DF.** 1996. Torque generation in the flagellar motor of *Escherichia coli*: evidence of a direct role for FliG but not for FliM or FliN. J. Bacteriol. **178**:223–231.
42. **McCarter LL.** 1994. MotX, the channel component of the sodium-type flagellar motor. J. Bacteriol. **176**:5988–5998.
43. **McCarter LL.** 1994. MotY, a component of the sodium-type flagellar motor. J. Bacteriol. **176**:4219–4225.
44. **Metcalf WW, Wanner BL.** 1993. Construction of new β-glucuronidase cassettes for making transcriptional fusions and their use with new methods for allele replacement. Gene **129**:17–25.
45. **Okabe M, Yakushi T, Kojima M, Homma M.** 2002. MotX and MotY, specific components of the sodium-driven flagellar motor, colocalize to the outer membrane in *Vibrio alginolyticus*. Mol. Microbiol. **46**:125–134.
46. **O'Neill J, Xie M, Hijnen M, Roujeinikova A.** 2011. Role of the MotB linker in the assembly and activation of the bacterial flagellar motor. Acta Crystallogr. D Biol. Crystallogr. **67**:1009–1016.
47. **Paul K, Gonzalez-Bonet G, Bilwes AM, Crane BR, Blair D.** 2011. Architecture of the flagellar rotor. EMBO J. **30**:2962–2971.
48. **Platzer J, Sterr W, Hausmann M, Schmitt R.** 1997. Three genes of a motility operon and their role in flagellar rotary speed variation in *Rhizobium meliloti*. J. Bacteriol. **179**:6391–6399.
49. **Poggio S, et al.** 2007. A complete set of flagellar genes acquired by horizontal transfer coexists with the endogenous flagellar system in *Rhodobacter sphaeroides*. J. Bacteriol. **189**:3208–3216.
50. **Poggio S, Osorio A, Dreyfus G, Camarena L.** 2005. The flagellar hierarchy of *Rhodobacter sphaeroides* is controlled by the concerted action of two enhancer-binding proteins. Mol. Microbiol. **58**:969–983.
51. **Poggio S, Osorio A, Dreyfus G, Camarena L.** 2002. The four different σ^{54} factors of *Rhodobacter sphaeroides* are not functionally interchangeable. Mol. Microbiol. **46**:75–85.
52. **Porter SL, et al.** 2011. Genome sequence of *Rhodobacter sphaeroides* strain WS8N. J. Bacteriol. **193**:4027–4028.
53. **Quandt J, Hynes MF.** 1993. Versatile suicide vectors which allow direct selection for gene replacement in Gram-negative bacteria. Gene **127**:15–21.
54. **Reboul CF, Andrews DA, Nahar MF, Buckle AM, Roujeinikova A.** 2011. Crystallographic and molecular dynamics analysis of loop motions unmasking the peptidoglycan-binding site in stator protein MotB of flagellar motor. PLoS One **6**:e18981. doi:10.1371/journal.pone.0018981.
55. **Reid SW, et al.** 2006. The maximum number of torque-generating units in the flagellar motor of *Escherichia coli* is at least 11. Proc. Natl. Acad. Sci. U. S. A. **103**:8066–8071.
56. **Senes A, Engel DE, DeGrado WF.** 2004. Folding of helical membrane proteins: the role of polar, GxxxG-like and proline motifs. Curr. Opin. Struct. Biol. **14**:465–479.
57. **Shah DS, Armitage JP, Sockett RE.** 1995. *Rhodobacter sphaeroides* WS8 expresses a polypeptide that is similar to MotB of *Escherichia coli*. J. Bacteriol. **177**:2929–2932.
58. **Shah DS, Sockett RE.** 1995. Analysis of the *motA* flagellar motor gene from *Rhodobacter sphaeroides*, a bacterium with a unidirectional, stop-start flagellum. Mol. Microbiol. **17**:961–969.
59. **Simon R, Priefer U, Pühler A.** 1983. A broad host range mobilization system for *in vivo* genetic engineering: transposon mutagenesis in Gram negative bacteria. Nat. Biotechnol. **1**:784–791.
60. **Sistrom WR.** 1962. The kinetics of the synthesis of photopigments in *Rhodopseudomonas spheroides*. J. Gen. Microbiol. **28**:607–616.
61. **Sockett RE, Foster JCA, Armitage JP.** 1990. Molecular biology of the *Rhodobacter sphaeroides* flagellum. FEMS Symp. **53**:473–479.
62. **Sommerlad SM, Hendrixson DR.** 2007. Analysis of the roles of FlgP and FlgQ in flagellar motility of *Campylobacter jejuni*. J. Bacteriol. **189**:179–186.
63. **Sowa Y, Berry RM.** 2008. Bacterial flagellar motor. Q. Rev. Biophys. **41**:103–132.
64. **Stolz B, Berg HC.** 1991. Evidence for interactions between MotA and MotB, torque-generating elements of the flagellar motor of *Escherichia coli*. J. Bacteriol. **173**:7033–7037.
65. **Suaste-Olmos F, et al.** 2010. The flagellar protein FliL is essential for swimming in *Rhodobacter sphaeroides*. J. Bacteriol. **192**:6230–6239.
66. **Terashima H, Fukuoka H, Yakushi T, Kojima S, Homma M.** 2006. The *Vibrio* motor proteins, MotX and MotY, are associated with the basal body of Na-driven flagella and required for stator formation. Mol. Microbiol. **62**:1170–1180.
67. **Terashima H, Kojima S, Homma M.** 2008. Flagellar motility in bacteria structure and function of flagellar motor. Int. Rev. Cell Mol. Biol. **270**:39–85.
68. **Tokuda H, et al.** 1988. Roles of the respiratory Na+ pump in bioenergetics of *Vibrio alginolyticus*. J. Biochem. **103**:650–655.
69. **Wilkinson DA, Chacko SJ, Venien-Bryan C, Wadhams GH, Armitage JP.** 2011. Regulation of flagellum number by FliA and FlgM and role in biofilm formation by *Rhodobacter sphaeroides*. J. Bacteriol. **193**:4010–4014.
70. **Yakushi T, Maki S, Homma M.** 2004. Interaction of PomB with the third transmembrane segment of PomA in the Na+-driven polar flagellum of *Vibrio alginolyticus*. J. Bacteriol. **186**:5281–5291.
71. **Yamaguchi S, et al.** 1986. Genetic evidence for a switching and energy-transducing complex in the flagellar motor of *Salmonella typhimurium*. J. Bacteriol. **168**:1172–1179.
72. **Yorimitsu T, Homma M.** 2001. Na(+)-driven flagellar motor of *Vibrio*. Biochim. Biophys. Acta **1505**:82–93.
73. **Yorimitsu T, Sato K, Asai Y, Kawagishi I, Homma M.** 1999. Functional interaction between PomA and PomB, the Na(+)-driven flagellar motor components of *Vibrio alginolyticus*. J. Bacteriol. **181**:5103–5106.
74. **Zhao R, Amsler CD, Matsumura P, Khan S.** 1996. FliG and FliM distribution in the *Salmonella typhimurium* cell and flagellar basal bodies. J. Bacteriol. **178**:258–265.
75. **Zhao R, Pathak N, Jaffe H, Reese TS, Khan S.** 1996. FliN is a major structural protein of the C-ring in the *Salmonella typhimurium* flagellar basal body. J. Mol. Biol. **261**:195–208.
76. **Zhou J, Blair DF.** 1997. Residues of the cytoplasmic domain of MotA essential for torque generation in the bacterial flagellar motor. J. Mol. Biol. **273**:428–439.
77. **Zhou J, Fazzio RT, Blair DF.** 1995. Membrane topology of the MotA protein of *Escherichia coli*. J. Mol. Biol. **251**:237–242.
78. **Zhou J, Lloyd SA, Blair DF.** 1998. Electrostatic interactions between rotor and stator in the bacterial flagellar motor. Proc. Natl. Acad. Sci. U. S. A. **95**:6436–6441.
79. **Zhou J, et al.** 1998. Function of protonatable residues in the flagellar motor of *Escherichia coli*: a critical role for Asp 32 of MotB. J. Bacteriol. **180**:2729–2735.